

## Induction of amphotericin B resistance in susceptible *Candida auris* by extracellular vesicles

Walton Chan <sup>a,\*</sup>, Franklin Wang-Ngai Chow <sup>b,a,\*</sup>, Chi-Ching Tsang <sup>c,a,\*</sup>, Xueyan Liu <sup>a</sup>, Weiming Yao <sup>a</sup>, Tony Tat-Yin Chan <sup>a</sup>, Gilman Kit-Hang Siu <sup>b</sup>, Alex Yat-Man Ho <sup>d</sup>, Kristine Shik Luk <sup>d</sup>, Susanna Kar-Pui Lau <sup>a</sup> and Patrick Chiu-Yat Woo <sup>e,f,a</sup>

<sup>a</sup>Department of Microbiology, Li Ka Shing Faculty of Medicine, The University of Hong Kong, Pokfulam, Hong Kong; <sup>b</sup>Department of Health Technology and Informatics, The Hong Kong Polytechnic University, Hungghom, Hong Kong; <sup>c</sup>School of Medical and Health Sciences, Tung Wah College, Homantin, Hong Kong; <sup>d</sup>Department of Pathology, Princess Margaret Hospital, Kwai Chung, Hong Kong; <sup>e</sup>PhD Program in Translational Medicine and Department of Life Sciences, National Chung Hsing University, Taichung, Taiwan; <sup>f</sup>The iEGG and Animal Biotechnology Research Center, National Chung Hsing University, Taichung, Taiwan

### ABSTRACT

Drug resistance derived from extracellular vesicles (EVs) is an increasingly important research area but has seldom been described regarding fungal pathogens. Here, we characterized EVs derived from a triazole-resistant but amphotericin B-susceptible strain of *Candida auris*. Nano- to microgram concentrations of *C. auris* EVs prepared from both broth and solid agar cultures could robustly increase the yeast's survival against both pure and clinical amphotericin B formulations in a dose-dependent manner, resulting in up to 16-fold changes of minimum inhibitory concentration. Meanwhile, this effect was not observed upon addition of these EVs to *C. albicans*, nor upon addition of *C. albicans* EVs to *C. auris*. No change in susceptibilities was observed upon EV treatment for fluconazole, voriconazole, micafungin, and flucytosine. Mass spectrometry indicated the presence of immunogenic-/drug resistance-implicated proteins in *C. auris* EVs, including alcohol dehydrogenase 1 as well as *C. albicans* Mp65-like and Xog1-like proteins in high quantities. Based on these observations, we propose a potential species-specific role for EVs in amphotericin B resistance in *C. auris*. These observations may provide critical insights into treatment of multidrug-resistant *C. auris*.

**ARTICLE HISTORY** Received 10 March 2022; Revised 30 June 2022; Accepted 30 June 2022

**KEYWORDS** *Candida auris*; extracellular vesicles; drug resistance; amphotericin B; solid media EV purification

### Introduction


*Candida auris* is a recently emerged pathogenic fungus described as a serious threat to global health by the US Centers for Disease Control and Prevention (CDC) due to its propensity for nosocomial outbreaks and multi-drug resistance [1]. The yeast was first discovered and described in 2009 from the external ear canal discharge of a patient in Japan [2]. Since then, infections caused by *C. auris* have been reported in six continents, with a crude mortality rate as high as 78%, depending on the geographic clades to which the aetiological *C. auris* isolates belong [3]. This novel fungal pathogen is also notorious for its persistence in the environment, especially in healthcare facilities due to its resistance to common disinfectants [4]. In Hong Kong, *C. auris* was first reported in June 2019 [5]. Identification of *C. auris* colonization in the city has since increased exponentially to over 200 incidents across four different local hospitals, especially

during July–December, 2020 when 85% of the positive isolations occurred; and *C. auris* detection continues to be reported from even the initial outbreak ward [5]. The isolate recovered from the index patient in Hong Kong belonged to the South Asian clade and was multi-drug resistant. In particular, it was resistant to fluconazole and was non-wild-type to all other triazole agents as well as the echinocandins caspofungin and anidulafungin; while it was only susceptible to amphotericin B and was wild-type to micafungin [5]. Recent reports have suggested that despite performing appropriate antifungal susceptibility testing, usage of corresponding clinical dosages can still result in treatment failure [6,7]. Therefore, further research into molecular and phenotypic mechanisms of drug resistance in *C. auris* is required.

Extracellular vesicles (EVs) collectively describe lipid bilayer-delimited secreted membrane vesicles [8]. They contain an assortment of cargo that vary

**CONTACT** Patrick Chiu-Yat Woo  pcywoo@hku.hk  PhD Program in Translational Medicine and Department of Life Sciences, National Chung Hsing University, 145 Xingda Road, South District, Taichung 402, Taiwan; Susanna Kar-Pui Lau  skplau@hku.hk  Department of Microbiology, Li Ka Shing Faculty of Medicine, The University of Hong Kong, 19/F, Block T, Queen Mary Hospital Compound, Pokfulam, Hong Kong

\*These authors contributed equally to this study.

 Supplemental data for this article can be accessed online at <https://doi.org/10.1080/22221751.2022.2098058>.

© 2022 The Author(s). Published by Informa UK Limited, trading as Taylor & Francis Group.

This is an Open Access article distributed under the terms of the Creative Commons Attribution-NonCommercial License (<http://creativecommons.org/licenses/by-nc/4.0/>), which permits unrestricted non-commercial use, distribution, and reproduction in any medium, provided the original work is properly cited.

according to the nutritional, metabolic, and environmental conditions of the cell. In mammalian and bacterial cells, EVs have been implicated in cell–cell communication [8–11], immunomodulation [12], and drug resistance [13,14]. For example, bacterial outer membrane vesicles (OMVs) can horizontally transfer carbapenemases and their corresponding genes [15,16], sequester antimicrobial peptides [17,18], and act as bacteriophage decoys [17]. Yet, the roles of EVs in fungi have not been as well-defined [8]. Thus far, drug resistance derived from fungal EVs has only been described in two studies; where EVs produced by *Candida albicans* and *Saccharomyces cerevisiae* were demonstrated to provide cellular protection against the antifungal drugs fluconazole and caspofungin, respectively [19, 20]. Notably, it was shown that the cargo of *S. cerevisiae* EVs included a number of cell wall modification enzymes; and therefore may have helped compensate for the inhibition of (1,3)- $\beta$ -D-glucan synthase upon caspofungin treatment [20]. Here, we show that EVs isolated from an amphotericin B-sensitive strain of *C. auris* can be back-added to increase the minimum inhibitory concentration (MIC) of amphotericin B by at least up to 16-fold in a dose-dependent manner. These findings may help explain the frequent failure to treat supposedly amphotericin B-susceptible *C. auris* with amphotericin B and may constitute a novel mechanism of resistance against the third class of effective antifungal drugs: the polyenes.

## Materials and methods

**Fungal strains.** *C. auris* strain Cau1901 was isolated from the index patient in Hong Kong from Princess Margaret Hospital in June 2019 [5]. The isolate was cryopreserved at  $-80^{\circ}\text{C}$  or maintained on Sabouraud dextrose agar (SDA; Difco, BD Diagnostics Systems, USA) supplemented with chloramphenicol (50  $\mu\text{g}/\text{mL}$ ; Calbiochem, USA) at  $37^{\circ}\text{C}$ . The reference strain *C. albicans* ATCC 90028 was obtained from the American Type Culture Collection (ATCC), USA. The quality control strain for susceptibility testing *C. parapsilosis* ATCC 22019<sup>T</sup> was obtained from the ATCC; strains *C. albicans* CNM-CL F8555 and *Pichia kudriavzevii* (synonym: *C. krusei*) CNM-CL-3403 were obtained from Statens Serum Institut (SSI), Denmark; and strain *P. kudriavzevii* NRRL Y-413 (= ATCC 6258) was obtained from the Agricultural Research Service (ARS) Culture Collection (NRRL), Department of Agriculture, USA.

**Isolation of fungal EVs.** (i) **Broth culture.** For both *C. auris* Cau1901 and *C. albicans* ATCC 90028, a single colony ( $\geq 1$  mm in diameter) on SDA was collected and transferred to 10 mL of Sabouraud dextrose broth (SDB, Sigma-Aldrich, USA) for growth at  $37^{\circ}\text{C}$  in a shaking incubator at 250 rpm. After 24 h of

incubation, 1 mL of the liquid culture was transferred to 1.25 L of fresh SDB in a 2 L conical flask for further growth at  $37^{\circ}\text{C}$  in a shaking incubator at 250 rpm. After a further 48 h of incubation, the liquid cultures were centrifuged at 15,000  $\times g$  for 15 min at  $4^{\circ}\text{C}$ , and the supernatant collected was vacuum filtered through 0.45  $\mu\text{m}$ -polyethersulphone (PES) membranes (Nalgene, USA). Every 1.25 L of filtered supernatant was concentrated via centrifugation at 3000  $\times g$  for 10 min at  $4^{\circ}\text{C}$  through a 100 kDa cellulose membrane concentrator (Merck, Germany) to a final volume of 25 mL. The concentrate was then collected for subsequent ultracentrifugation. (ii) **Agar plate culture.** For both *C. auris* Cau1901 and *C. albicans* ATCC 90028, fungal material was collected using a 10  $\mu\text{L}$  inoculation loop and resuspended in 30 mL of phosphate-buffered saline (PBS; Oxoid, UK). After centrifugation at 3000  $\times g$  for 5 min, the supernatant was collected and vacuum filtered through 0.45  $\mu\text{m}$ -PES membrane. The filtrate was then collected for subsequent ultracentrifugation. (iii) **EV isolation and purification.** For both supernatant concentrate collected from broth cultures and filtrate collected from agar plate cultures, ultracentrifugation was performed at 100,000  $\times g$  for 1.5 h at  $4^{\circ}\text{C}$  using the Optima XE (Beckman Coulter, USA) ultracentrifuge equipped with a SW32-Ti rotor (Beckman Coulter). Next, the pellets were resuspended in PBS and then subjected to particle separation via layered iodixanol (OptiPrep, Stemcell Technologies, Canada) density gradient ultracentrifugation at 100,000  $\times g$  for 16 h at  $4^{\circ}\text{C}$ . The separated layers of different densities were then collected sequentially, and each fraction was washed with PBS by ultracentrifugation at 100,000  $\times g$  for 1.5 h at  $4^{\circ}\text{C}$  twice. The density of each fraction was calculated from the measurement using a refractometer.

**Isolation of human reticulocyte EVs.** Human red blood cell EVs were isolated according to Usman and colleagues' protocol [21].

**EV quantification and measurements.** Nanoparticle tracking analysis (NTA) was performed for each iodixanol fraction obtained using the ZetaView PMX-220 TWIN Laser system (Particle Metrix, Germany) for size and particle number quantification. Briefly, for each iodixanol fraction 1  $\mu\text{L}$  of the solution was diluted in 10 mL of PBS prior to NTA for size and concentration and 1 mL of each diluted sample was used for the analysis. Each experiment was recorded at 11 random positions capturing 100–1000 particles (the “green” range) with 75 arbitrary units of sensitivity and a shutter speed of 0.01 s. All other parameters were kept at the manufacturer's default settings. The protein content of each iodixanol fraction was also measured using the Pierce BCA Protein Assay Kit (Thermo Scientific, USA) according to the manufacturer's protocol. Briefly, 10  $\mu\text{L}$  of each undiluted iodixanol fraction was added to an alkaline reagent mix

composed of reagent A and reagent B and then incubated for 30 min at 37°C. The resulting colour change was measured using the VICTOR Multilabel Plate Reader (Perkin Elmer, USA) and quantified against a standard bovine serum albumin (Thermo Scientific) protein curve. Measurements were performed in duplicate and averaged.

**Transmission electron microscopy (TEM).** Each iodixanol fraction was examined under TEM for particle visualization. Briefly, 1 µL of each iodixanol fraction was diluted in 5 µL of autoclaved Milli-Q water. Samples were negatively stained with 2.5% uranyl acetate and analysed using the transmission electron microscope Phillips CM100 (Philips Electron Optics, the Netherlands) equipped with the Tengra charge-coupled device (CCD) camera (Olympus Soft Imaging Solutions, Germany). At least three grid positions were interrogated per sample, and two independent experiments were performed.

**Protein profile analysis.** For each iodixanol fraction, 20 µL of the solution was subjected to sodium dodecyl sulphate–polyacrylamide gel electrophoresis (SDS–PAGE) under a reducing condition at 120 V using 12% Mini-PROTEAN TGX precast gels (Bio-Rad, USA) for 30 min. The separated proteins were then stained using the Pierce Silver Stain for Mass Spectrometry (Thermo Scientific) kit according to the manufacturer's instructions. The 25–35 kDa band from Fraction F6 (1.087 g/L iodixanol) from the gel was excised, purified, and trypsin-digested at the Centre for PanorOmic Sciences (CPOS) Proteomics and Metabolomics Core at the Li Ka Shing Faculty of Medicine of The University of Hong Kong (HKU). The peptides were identified via liquid chromatography–mass spectrometry (LC–MS) using the timsTOF Pro mass spectrometer (Bruker Daltonics, Germany) and results were analysed using MaxQuant v1.16.17 (Max-Planck-Institute of Biochemistry, Germany). The resulting protein profile was subject to Gene Ontology (GO) analysis using the *Candida* Genome Database Gene Ontology Slim Mapper [22].

**Antifungal susceptibility testing.** Susceptibility testing experiments were conducted following the European Committee on Antimicrobial Susceptibility Testing (EUCAST) guidelines for yeast using the broth microdilution method [23]. Briefly, 100 µL of 2× RPMI 1640 medium (Gibco, USA) supplemented with 2% glucose (VWR Chemicals, United Kingdom), buffered with 3-(N-morpholino)propanesulphonic acid (MOPS; Merck KGaA, Germany), and adjusted to pH 7.0 using NaOH (Sigma Aldrich) with various drug dilutions (all drugs were obtained from Target-Mol [USA] except that pure amphotericin B powder was obtained from Cayman Chemical [USA], liposomal amphotericin B [AmBisome] from Gilead Sciences [USA] and amphotericin B deoxycholate from Bristol-Myers Squibb [USA]) was added to

each well of a flat-bottom tissue-treated 96 well plate (Eppendorf, Germany). Next, EVs (0, 1 or 5 µg in 10 µL of PBS) were added to each well, followed by inoculation with 100 µL of *C. auris* Cau1901 or *C. albicans* ATCC 90028 adjusted to 0.5 McFarland standard ( $1-5 \times 10^5$  cells/mL). 10 µL of PBS was added to each positive control well to ensure that the observed effects were not due to the dilution of growth media. Measurements of growth were read using the VICTOR Multilabel Plate Reader at 405 nm 24 h post-inoculation. The MIC was defined as 50% inhibition of growth for the triazoles (fluconazole and voriconazole), echinocandins (anidulafungin and micafungin), and flucytosine, while the MIC for amphotericin B was defined as 90% inhibition of growth. Apart from the addition of EVs into susceptibility testing, yeast cell lysates were also used to serve as controls. Briefly, a loopful of cells were resuspended in 500 µL of PBS supplemented with the cComplete, Mini, EDTA-free Protease Inhibitor Cocktail (Roche Diagnostics, Switzerland) containing 100 µL of 425–600 µm unwashed glass beads (Sigma-Aldrich). The cells were then mechanically disrupted using the TissueLyser II (Qiagen, Germany) for 1 min at 30 Hz. The lysed cell suspensions were then centrifuged at 3000 ×g for 10 min at 4°C; and the supernatant was collected and their protein content was quantified using the Pierce BCA Protein Assay Kit.

## Results

**Morphology and characterization of *C. auris* EVs.** *C. auris* EVs could be isolated from both broth and solid agar cultures and were similarly sized, though mainly localized in separate fractions upon density ultracentrifugation (Figure 1). TEM, NTA, and BCA all confirmed that broth culture EVs were found in F4–F7, while agar culture EVs were found in F3–F8 (Figure 1). The median sizes for broth culture- and agar culture-derived EVs were 215 and 207 nm, respectively, according to NTA (Figure 1(a)) and were in accordance with the sizes of various fungal EVs reported thus far [8, 24–26]. The purity of the preparation was confirmed through negative staining TEM using uranyl acetate, which showed a lack of protein aggregates and contaminating material (Figure 1(c)). Here, the classically described concave-cupped EVs [27] were successfully isolated from broth and agar cultures of *C. auris*.

An SDS–PAGE for the iodixanol-separated fractions was performed to separate *C. auris* EV proteins by mass. The protein amounts as measured by BCA correlated with the intensity of the bands on the silver-stained gel (Figure 2(a)). Additionally, a distinct band was found around ~25–35 kDa in the fractions with the highest concentration of EVs in both broth (F5) and agar culture (F6) preparations. This band



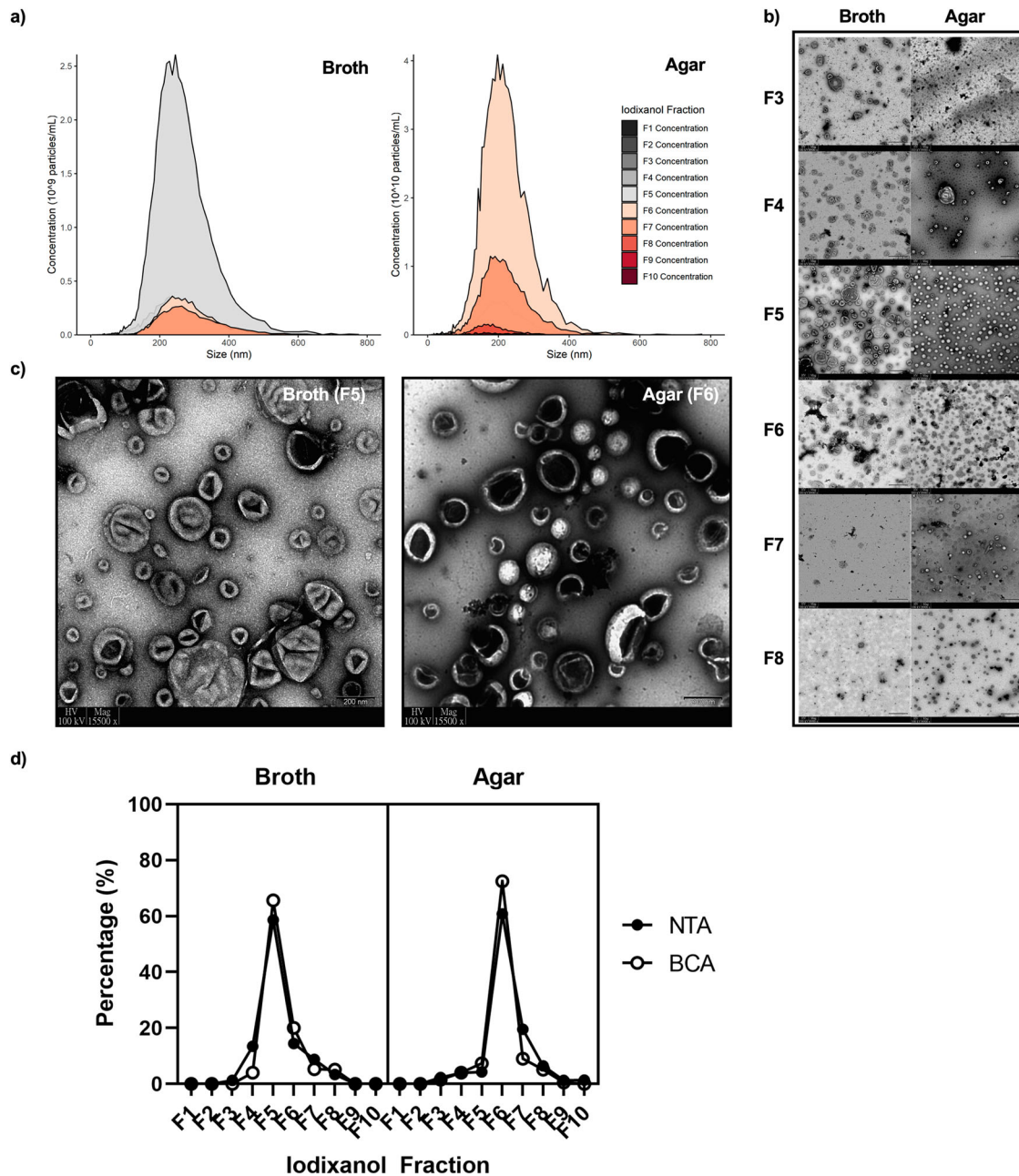


**Figure 1.** Differences and similarities of extracellular vesicles (EVs) derived from *Candida auris* using two culture methods. F3–F8 fractions correspond to densities of 1.044, 1.061, 1.065, 1.087, 1.101, and  $1.127 \pm 0.01$  g/L, respectively. (a) Nanoparticle tracking analysis (NTA) of all separated iodixanol fractions from broth and agar cultures,  $n = 3$ . (b) Transmission electron microscopy (TEM) of separated iodixanol fractions from broth and agar cultures. Three grid positions were interrogated per sample,  $n = 3$ . Scale bars = 200 nm. (c) Representative TEM micrographs of the fractions containing the highest concentration of EVs. (d) Pooled comparison of the relative amount of EVs found in each fraction measured through NTA and bicinchoninic acid protein measurement assay,  $n = 3$ .

from F6 of agar culture preparation was excised and subjected to LC–MS analysis. The resulting protein profile returned 49 proteins with at least one unique peptide detected (Supplementary Data File 1). To infer whether patterns of biological significance exist, the list underwent GO analysis for cellular location, biological processes, and molecular function (Figure S1). The GO analysis was generally nondescript and indicated most proteins were of cytoplasmic and mitochondrial origins (25/49 and 13/49, respectively).

These proteins were usually associated with enzymatic function and not structural (Figure S1). Because GO analysis did not reveal obvious clues to *C. auris* EV function, a manual approach to investigating the protein list was taken. The list was first narrowed to appropriate sizes (25–50 kDa) and five proteins with high protein intensities (iBAQ > 5,000, Figure 2(b)) were identified. These included alcohol dehydrogenase 1, elongation factor 1 $\alpha$ , phosphoglycerate kinase, and two uncharacterized proteins (A0A2H0ZTX6

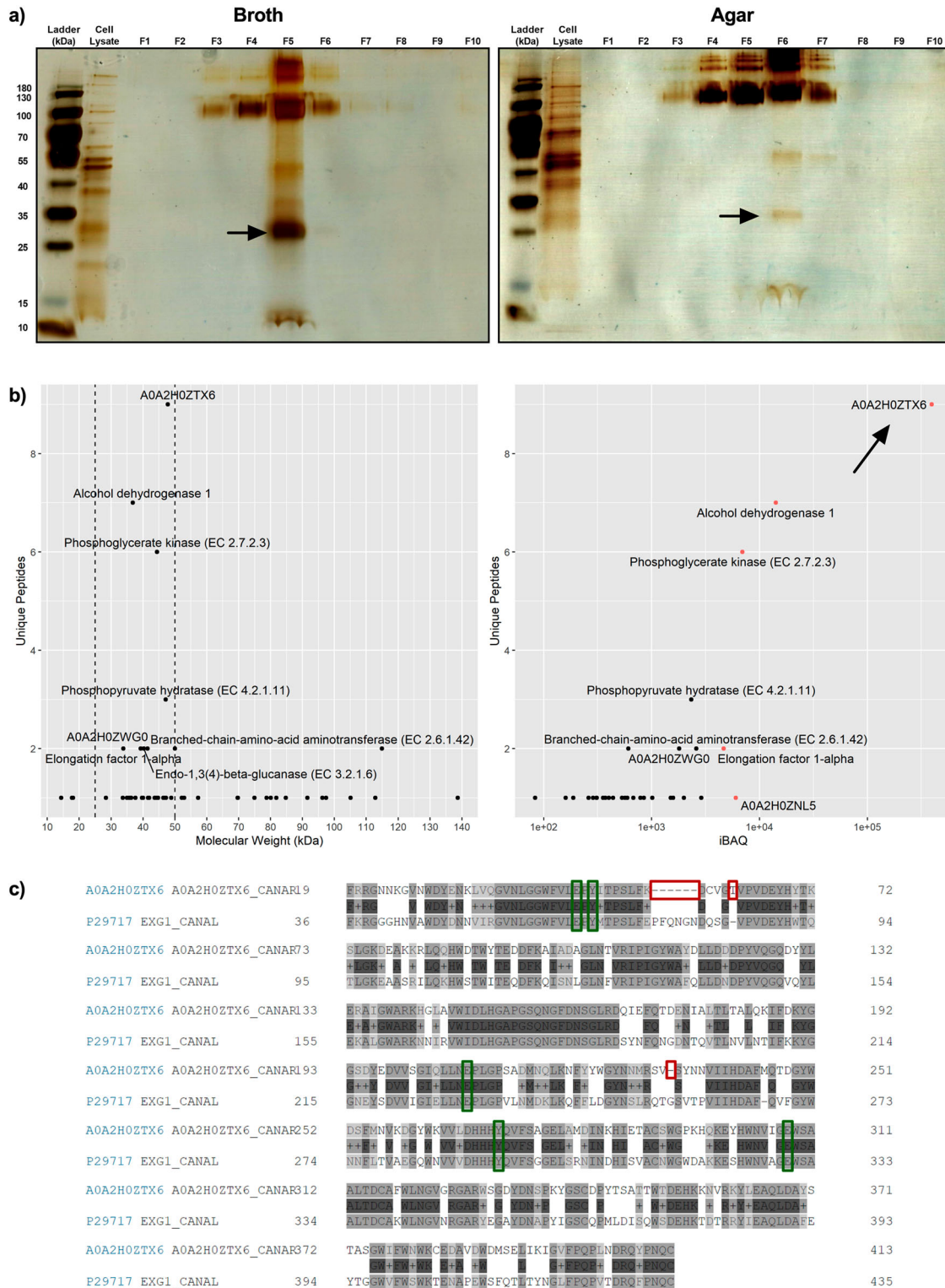


**Figure 2.** Proteomic analysis of abundant small proteins in *Candida auris* extracellular vesicles reveals immunogenic and drug-related cargo. (a) Representative silver-stained SDS–PAGE of broth and agar-derived density gradient-separated fractions,  $n = 2$ . (b) Detailed analysis of protein list obtained using tandem liquid chromatography mass spectrometry of excised 25–35 kDa band. Proteins were first separated by molecular weight (25–50 kDa, left), then plotted against protein intensity (right). The top 5 proteins in iBAQ are highlighted red. (c) Aligned protein sequences of *C. auris* A0A2H0ZTX6 (above) and *C. albicans* Xog1 (below, P29717; alternative name: EXG1). Green boxes indicate conserved glycosylation sites and/or active sites, red boxes indicate insertions or deletions for *C. auris* A0A2H0ZTX6 when compared with *C. albicans* Xog1.

and A0A2H0ZNI5). A0A2H0ZTX6 and A0A2H0ZNI5 shared 61.4% and 60.9% amino acid similarity to *C. albicans* glucosidase Xog1 and a

major antigen mannoprotein Mp65, respectively. Amongst the five proteins identified, A0A2H0ZTX6 had both the highest protein intensity and number

of unique peptides found. All described active sites and substrate binding domains in *C. albicans* Xog1 were found to be conserved in *C. auris* Xog1 (Figure 2(c)).

**Effect of *C. auris* EV treatment on antifungal susceptibility.** Drug susceptibility testing was performed for *C. auris* Cau1901 and *C. albicans* ATCC 90028 against a panel of antifungal drugs to establish baseline susceptibility prior to EV addition. Similar to most isolates in *C. auris* clade I [28], *C. auris* Cau1901 exhibited significant levels of resistance towards the triazole class of antifungals (MIC >128 µg/mL for fluconazole and MIC >16 µg/mL for voriconazole; Figures S2a–b). On the other hand, MICs for amphotericin B, flucytosine, and micafungin were 1, 0.25, and ≤0.03 µg/mL, respectively (Figure 3(a) and Figures S2c–d).

Given the antifungal resistance profile of *C. auris* Cau1901, we asked whether EVs derived from this multidrug-resistant organism could be a mechanism of drug resistance. Because a close correlation between the relative protein quantity and EV concentration was found (Figure 1(d)), protein quantity was used as a surrogate for EV concentration. *C. auris* EVs derived from agar and broth cultures were added to microdilution in vitro cultures of *C. auris* using human reticulocyte EVs as a control for fluconazole and voriconazole first. No difference in MIC was observed for the triazoles after the back-addition of EVs (Figure S2a–b). As flucytosine and micafungin are used in clinical practice against *C. auris* infection, an increased concentration of agar-derived EVs was added to observe if any effect was present. Still, no difference from the control was observed (Figure S2c–d).

On the other hand, the MICs for the pure pharmaceutical formulation and both of the clinical formulations of amphotericin B were increased upon EV addition in *C. auris* in a dose dependent manner (Figure 3). As little as 0.1 µg of EVs was able to quadruple the MIC and allowed for *C. auris* survival at 2 µg/mL of pure amphotericin B. Meanwhile, the addition of ≥1 µg of EVs allowed for robust survival of *C. auris* at 16 µg/mL of pure amphotericin B, suggesting a ≥16-fold increase in MIC (Figure 3(a)). To expand the significance of our findings, we performed the same experiments on two clinical formulations of amphotericin B. Similar potency was observed when adding *C. auris* EVs to plates containing amphotericin B deoxycholate, a formulation with increased solubility in water (Figure 3(b)). Most surprisingly, this resistance effect persisted when *C. auris* supplemented with EVs was treated against amphotericin B encapsulated in hydrogenated soy phosphatidylcholine bilayer liposomes (liposomal amphotericin B, Figure 3(c)), though no difference in MICs was observed between the control and the

lowest concentration treatment group (addition of 0.1 µg EVs). Although official breakpoints have not yet been established for *C. auris*, an MIC ≥2 µg/mL alters the classification of *C. auris* Cau1901 from “wild-type” to “non-wild-type” against amphotericin B based on the tentative EUCAST epidemiological cut-off value (ECOFF) for *C. auris* [29] or from sensitive to resistant against this drug according to the tentative breakpoint published by the CDC [30]. On the other hand, when an equivalent protein amount of EVs derived from a commonly studied, amphotericin B-susceptible strain of *C. albicans* was added to wells containing *C. auris* and amphotericin B, a drastically reduced increase in MICs was observed (Figure S3). Moreover, the addition of 3 µg of *C. auris* EVs to *C. albicans* also did not increase its MICs in any of the formulations of amphotericin B (Figure 3).

## Discussion

EVs were isolated and purified from both broth and agar cultures of the newly emerged fungal pathogen *C. auris* in this study. Given the relative novelty of the agar culture method compared to broth culture, we first assessed whether differences exist in the EVs produced by both methods. In addition to producing comparatively greater yield, decreased labour and material cost, as well as reduced biosafety risk [26], EV collection from colonies grown on a solid matrix may constitute a better physiological model for *C. auris* as a skin colonizer/pathogen. *C. auris* EVs were found to be slightly larger than previously reported EVs from other *Candida* species (100–200 nm) [24] (Figure 1(a)), though differences in preparation, strains, and measuring methods (dynamic light scattering vs NTA) may contribute to this phenomenon. Furthermore, NTA has been found to favour larger sized particles in a heterogeneous population [31]. Thus, *C. auris* EVs fall within expected deviation for typical fungal EVs.

Proteins in *C. auris* EVs may provide insight on drug resistance-related EV function and possible avenues for immunotherapy. Five proteins were found in abundant quantities in *C. auris* EVs (Figure 2(b)). Three of them (alcohol dehydrogenase 1, A0A2H0ZTX6, and A0A2H0ZNI5) are suspected to be immunogenic [32, 33]. The two uncharacterized proteins were also identified to be homologues of *C. albicans* β-1,3-exoglucanase Xog1 and β-1,3-endoglucanase mannoprotein Mp65, respectively, which are major components of the *C. albicans* secretome. Xog1 is a hyphal-specific virulence factor which has been implicated in transporting glucan across membranes for biofilm formation, and thus may play some role in biofilm-derived drug resistance [33]. In a brief analysis, all of the glycosylation sites and substrate binding domains were found to be



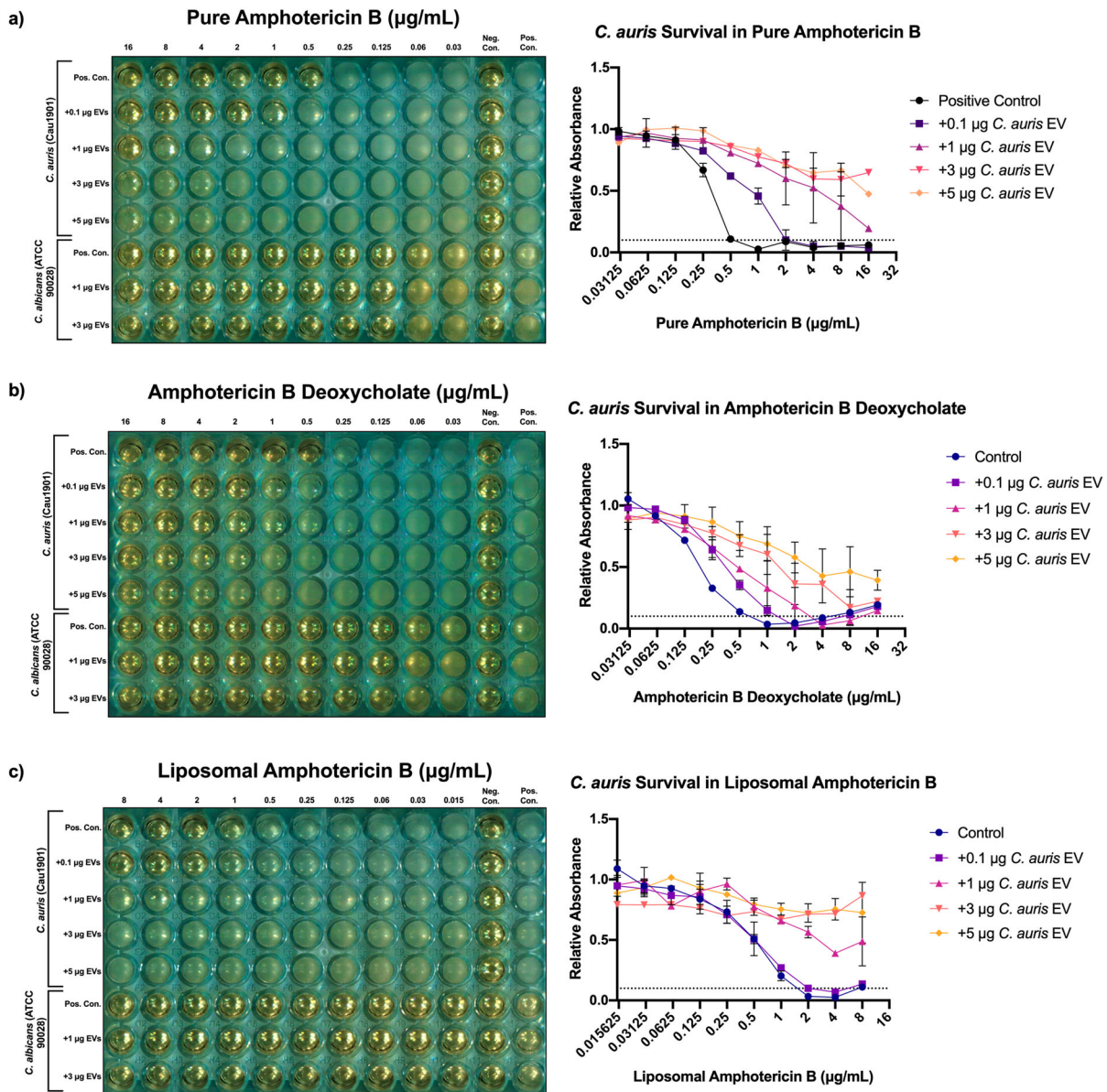


**Figure 3.** The addition of *Candida auris* extracellular vesicles to in vitro *C. auris* cultures increases their resistance to amphotericin B in a dose-dependent manner, but not *C. albicans*. Left: Representative European Committee on Antimicrobial Susceptibility Testing (EUCAST) antifungal susceptibility testing (AFST) broth microdilution plate incubated with treatment groups,  $n = 3$ . Right: mean relative absorbance of AFST plates inoculated with *C. auris* Cau1901 measured at 450 nm after 24 h,  $n = 3$ . (a) Pure amphotericin B. (b) Water soluble amphotericin B deoxycholate. (c) Liposomal amphotericin B.

conserved among the two proteins. Importantly, *C. albicans* Xog1 is also the target for host antimicrobial peptide cathelicidin LL-37 which plays a key role in the antimicrobial barrier function in skin and epithelial surfaces [32]. Therefore, the presence of a Xog1-like protein in *C. auris* EVs may indicate a role for innate immune evasion through the release of EVs and may contribute to the success of *C. auris* as a skin colonizer. Despite abundant secretion in a soluble protein form and presence in biofilm EVs, however, Xog1 is absent in *C. albicans* yeast EVs and biofilm cell lysate [25]. In addition, certain deletions and an insertion were detected in *C. auris*' A0A2H0ZTX6 when compared with *C. albicans*' Xog1. These differentiations may account for the species-specific differences we observed when

performing our susceptibility testing. Meanwhile, the presence of a homologue of an immunodominant mannoprotein Mp65 may also indicate the potential for *C. auris* EVs in immunotherapy. In *C. albicans*, both the mannosylated Mp65 and recombinant Mp65 without a mannan moiety induce a robust Th1 cytokine pattern in antigen-presenting cells and led to T cell activation [34]. This, combined with observations that mannoproteins and mannans primarily drive the host innate immune response to *C. auris*, suggested that *C. auris* EVs could be further investigated for their immunogenicity and vaccine potential.

*C. auris* EVs modulate amphotericin B susceptibilities in a species-specific manner. In this study, it was demonstrated that EVs from *C. auris* were able

to decrease *C. auris* sensitivities towards amphotericin B, but not *C. albicans* (Figure 3). Conversely, *C. albicans* EVs were unable to affect *C. auris* MICs to amphotericin B (Figure S3). We hypothesize that this phenomenon may individually or synergistically work in three possible ways. First, *C. auris* EVs may modulate susceptibility to amphotericin B by drug sequestration or competitive binding. Amphotericin B demonstrates high binding affinity to the cell wall sterol ergosterol. As fungal EV membranes are largely composed of ergosterol [8, 35], it stands to reason that *C. auris* EVs may competitively bind amphotericin B molecules and reduce bioavailability of the drug, leading to greater fungal survival. However, the same effect of increased amphotericin B resistance was not observed for the addition of *C. albicans* EVs to *C. auris* (Figure S3), which was puzzling since membranes of *C. albicans* EVs are also largely composed of ergosterol [35]. Such an observation suggests that an alternative or supplementary model to this bioavailability theory is needed to explain how *C. auris* EVs modulate amphotericin B resistance. The second possible way in which *C. auris* EVs modulate amphotericin B resistance may be their role as a supplementary source of ergosterol to the cell. As suggested by Zarnowski et al., a similar composition of membrane proteins, lipids, and polysaccharides between the source cell and EVs combined with knowledge that EVs can bind cell walls and be internalized in *C. albicans* suggest that *C. auris* EVs can act as supplementary membrane material through membrane fusion [19]. The addition of a supplementary source of ergosterol from *C. auris* EVs may aid to stabilize the membrane by maintaining fluidity and help the fungus survive in the presence of amphotericin B. Indeed, this may also explain why *C. auris* EVs increased MIC to amphotericin B in *C. auris* cultures only but not *C. albicans* as the inter-species incorporation of a different membrane composition is less likely to occur. The presence of structural synthesis enzymes in *C. auris* EVs may represent the third possible way for how *C. auris* EVs modulate resistance to amphotericin B. The enrichment of compensatory cell wall remodelling enzymes in EVs from the distantly related model yeast *S. cerevisiae* such as glucan synthase subunit Fks1 and chitin synthase Chs3 suggests that a similar mechanism may exist for *C. auris* EVs. Indeed, one of the most highly expressed proteins in our EV samples was a Xog1 homologue (Figure 2(b)), which in *C. albicans* helps maintain cell wall integrity through  $\beta$ -glucan modifications [33]. Notably, thicker cell walls due to increased  $\beta$ -glucan composition in *C. tropicalis* have been associated with amphotericin B resistance [36], so structural enzymes present in EVs may act to repair or prevent membrane damage. Further work

such as quantitative proteomic analysis on whole EV samples will help elucidate this answer.

Our research suggests that the discrepancies observed between in vitro antifungal susceptibility testing dosages and clinical dosages in *C. auris* infections can be partly attributed to the release of EVs. By extension, novel drugs targeting EV trafficking such as turbinmicin [37] may find synergistic efficacy when combined with existing antifungal drugs. Further research will be required to explore the potential clinical impact of our findings and whether other antimicrobial threats utilize similar mechanisms to evade drugs.

## Acknowledgements

We thank the Department of Pathology, HKU for the use of their nanoparticle tracking analysis machine and technical expertise; the Electron Microscope Unit, HKU for their technical support and assistance in sample preparation for TEM; and the Proteomics and Metabolomics Unit, HKU for their technical support and assistance in performing LC-MS.

## Disclosure statement

Patrick Chiu-Yat Woo has provided scientific advisory/laboratory services for Gilead Sciences, Incorporated; International Health Management Associates, Incorporated; Merck & Corporation, Incorporated; Micologia Molecular S.L. and Pfizer, Incorporated. The other authors report no conflict of interest. The funding sources had no role in study design, data collection, analysis, interpretation, or writing of the report. The authors alone are responsible for the content and the writing of the manuscript.

## Funding

This work was partly supported by the General Research Fund, Research Grants Council, University Grants Committee; as well as the framework of the Higher Education Sprout Project by the Ministry of Education (MOE-111-S-023-A) in Taiwan.

## Ethics statement

The use of clinical *C. auris* isolate in this study and leftover human blood specimens was approved by the Institutional Review Board of The University of Hong Kong/Hospital Authority Hong Kong West Cluster (UW 16-365).

## ORCID

Walton Chan  <http://orcid.org/0000-0003-0909-8414>  
 Franklin Wang-Ngai Chow  <http://orcid.org/0000-0003-1275-2464>  
 Chi-Ching Tsang  <http://orcid.org/0000-0001-6705-2866>  
 Xueyan Liu  <http://orcid.org/0000-0003-3756-9172>  
 Weiming Yao  <http://orcid.org/0000-0002-6430-1211>



Tony Tat-Yin Chan  <http://orcid.org/0000-0003-3982-1597>

Gilman Kit-Hang Siu  <http://orcid.org/0000-0002-4354-3393>

Susanna Kar-Pui Lau  <http://orcid.org/0000-0002-1383-7374>

Patrick Chiu-Yat Woo  <http://orcid.org/0000-0001-9401-1832>

## References

- [1] Chaabane F, Graf A, Jequier L, et al. Review on antifungal resistance mechanisms in the emerging pathogen *Candida auris*. *Front Microbiol.* **2019**;10:2788.
- [2] Satoh K, Makimura K, Hasumi Y, et al. *Candida auris* sp. nov., a novel ascomycetous yeast isolated from the external ear canal of an inpatient in a Japanese hospital. *Microbiol Immunol.* **2009**;53(1):41–44.
- [3] Chen J, Tian S, Han X, et al. Is the superbug fungus really so scary? A systematic review and meta-analysis of global epidemiology and mortality of *Candida auris*. *BMC Infect Dis.* **2020**;20(1):827.
- [4] Ku TSN, Walraven CJ, Lee SA. *Candida auris*: disinfectants and implications for infection control. *Front Microbiol.* **2018**;9:726.
- [5] Woo PCY, Tsang C-C, Lau SKP. Antifungal resistance: an emerging battlefield. *Future Microbiol.* **2020**;15(8):571–574.
- [6] Vazquez JA, Arganoza MT, Boikov D, et al. Stable phenotypic resistance of *Candida* species to amphotericin B conferred by preexposure to subinhibitory levels of azoles. *J Clin Microbiol.* **1998**;36(9):2690–2695.
- [7] Alatoom A, Sartawi M, Lawlor K, et al. Persistent candidemia despite appropriate fungal therapy: first case of *Candida auris* from the United Arab Emirates. *Int J Infect Dis.* **2021**;70:36–37.
- [8] Rizzo J, Rodrigues ML, Janbon G. Extracellular vesicles in fungi: past, present, and future perspectives. *Front Cell Infect Microbiol.* **2020**;10:346.
- [9] Paolicelli RC, Bergamini G, Rajendran L. Cell-to-cell communication by extracellular vesicles: focus on microglia. *Neuroscience.* **2019**;405:148–157.
- [10] Crewe C, Joffin N, Rutkowski JM, et al. An endothelial-to-adipocyte extracellular vesicle axis governed by metabolic state. *Cell.* **2018**;175(3):695–708.e13.
- [11] Chow FW-N, Koutsovoulos G, Ovando-Vázquez C, et al. Secretion of an argonaute protein by a parasitic nematode and the evolution of its siRNA guides. *Nucleic Acids Res.* **2019**;47(7):3594–3606.
- [12] Kuipers ME, Hokke CH, Smits HH, et al. Pathogen-derived extracellular vesicle-associated molecules that affect the host immune system: an overview. *Front Microbiol.* **2018**;9:2182.
- [13] Namee NM, O'Driscoll L. Extracellular vesicles and anti-cancer drug resistance. *Biochim Biophys Acta Rev Cancer.* **2018**;1870(2):123–136.
- [14] Xavier CPR, Caires HR, Barbosa MAG, et al. The role of extracellular vesicles in the hallmarks of cancer and drug resistance. *Cells.* **2020**;9(5):1141.
- [15] Jin JS, Kwon SO, Moon DC, et al. *Acinetobacter baumannii* secretes cytotoxic outer membrane protein A via outer membrane vesicles. *PLoS ONE.* **2011**;6(2):e17027.
- [16] Rumbo C, Fernández-Moreira E, Merino M, et al. Horizontal transfer of the OXA-24 carbapenemase gene via outer membrane vesicles: a new mechanism of dissemination of carbapenem resistance genes in *Acinetobacter baumannii*. *Antimicrob Agents Chemother.* **2011**;55(7):3084–3090.
- [17] Manning AJ, Kuehn MJ. Contribution of bacterial outer membrane vesicles to innate bacterial defense. *BMC Microbiol.* **2011**;11:258.
- [18] Kulkarni HM, Swamy Ch V, Jagannadham MV. Molecular characterization and functional analysis of outer membrane vesicles from the antarctic bacterium *Pseudomonas syringae* suggest a possible response to environmental conditions. *J Proteome Res.* **2014**;13(3):1345–1358.
- [19] Zarnowski R, Sanchez H, Covelli AS, et al. *Candida albicans* biofilm-induced vesicles confer drug resistance through matrix biogenesis. *PLoS Biol.* **2018**;16(10):e2006872.
- [20] Zhao K, Bleackley M, Chisanga D, et al. Extracellular vesicles secreted by *Saccharomyces cerevisiae* are involved in cell wall remodelling. *Commun Biol.* **2019**;2(1):305.
- [21] Usman WM, Pham TC, Kwok YY, et al. Efficient RNA drug delivery using red blood cell extracellular vesicles. *Nat Commun.* **2018**;9(1):2359.
- [22] Costanzo MC, Arnaud MB, Skrzypek MS, et al. The *Candida* Genome Database: facilitating research on *Candida albicans* molecular biology. *FEMS Yeast Res.* **2006**;6(5):671–684.
- [23] Arendrup MC, Meletiadis J, Mouton JW, et al. EUCAST Definitive Document E.Def 7.3.2 Method for the Determination of Broth Dilution Minimum Inhibitory Concentrations of Antifungal Agents for Yeasts 2020. Available from: [https://www.eucast.org/fileadmin/src/media/PDFs/EUCAST\\_files/AFST/Files/EUCAST\\_E\\_Def\\_7.3.2\\_Yeast\\_testing\\_definitive\\_revised\\_2020.pdf](https://www.eucast.org/fileadmin/src/media/PDFs/EUCAST_files/AFST/Files/EUCAST_E_Def_7.3.2_Yeast_testing_definitive_revised_2020.pdf).
- [24] Karkowska-Kuleta J, Kulig K, Karnas E, et al. Characteristics of extracellular vesicles released by the pathogenic yeast-like fungi *Candida glabrata*, *Candida parapsilosis* and *Candida tropicalis*. *Cells.* **2020**;9(7):1722.
- [25] Dawson CS, Garcia-Ceron D, Rajapaksha H, et al. Protein markers for *Candida albicans* EVs include claudin-like Sur7 family proteins. *J Extracell Vesicles.* **2020**;9(1):1750810.
- [26] Reis FCG, Borges BS, Jozefowicz LJ, et al. A novel protocol for the isolation of fungal extracellular vesicles reveals the participation of a putative scramblase in polysaccharide export and capsule construction in *Cryptococcus gattii*. *mSphere.* **2019**;4(2):e00080–19.
- [27] Théry C, Amigorena S, Raposo G, et al. Isolation and characterization of exosomes from cell culture supernatants and biological fluids. *Curr Protoc Cell Biol.* **2006**;30(1):3.22.1–3.22.29.
- [28] Muñoz JF, Gade L, Chow NA, et al. Genomic insights into multidrug-resistance, mating and virulence in *Candida auris* and related emerging species. *Nat Commun.* **2018**;9(1):5346.
- [29] Arendrup MC, Prakash A, Meletiadis J, et al. Comparison of EUCAST and CLSI reference microdilution MICs of eight antifungal compounds for *Candida auris* and associated tentative epidemiological cutoff values. *Antimicrob Agents Chemother.* **2017**;61(6):e00485–17.
- [30] Centers for Disease Control and Prevention. (2020). *Candida auris*. *Laboratorians and Health Professionals.*

- Antifungal Susceptibility Testing and Interpretation. [2021-10-03]. Available from: <https://www.cdc.gov/fungal/candida-auris/c-auris-antifungal.html>.
- [31] Krueger AB, Carnell P, Carpenter JF. Characterization of factors affecting nanoparticle tracking analysis results with synthetic and protein nanoparticles. *J Pharm Sci*. 2016;105(4):1434–1443.
- [32] Tsai P-W, Yang C-Y, Chang H-T, et al. Characterizing the role of cell-wall  $\beta$ -1,3-exoglucanase Xog1p in *Candida albicans* adhesion by the human antimicrobial peptide LL-37. *PLoS ONE*. 2011;6(6):e21394.
- [33] Sorgo AG, Heilmann CJ, Brul S, et al. Beyond the wall: *Candida albicans* secret(e)s to survive. *FEMS Microbiol Lett*. 2013;338(1):10–17.
- [34] Pietrella D, Lupo P, Rachini A, et al. A *Candida albicans* mannoprotein deprived of its mannan moiety is efficiently taken up and processed by human dendritic cells and induces T-cell activation without stimulating proinflammatory cytokine production. *Infect Immun*. 2008;76(9):4359–4367.
- [35] Vargas G, Honorato L, Guimarães AJ, et al. Protective effect of fungal extracellular vesicles against murine candidiasis. *Cell Microbiol*. 2020;22(10):e13238.
- [36] Mesa-Arango AC, Rueda C, Román E, et al. Cell wall changes in amphotericin B-resistant strains from *Candida tropicalis* and relationship with the immune responses elicited by the host. *Antimicrob Agents Chemother*. 2016;60(4):2326–2335.
- [37] Zhao M, Zhang F, Zarnowski R, et al. Turbinmicin inhibits *Candida* biofilm growth by disrupting fungal vesicle-mediated trafficking. *J Clin Invest*. 2021;131(5):e145123.